Electronic Supplementary Material (ESI) for RSC Advances.

Section – 1

Effect of Size on Mechanical Properties of Bonded Bilayer Germanene Sheets:

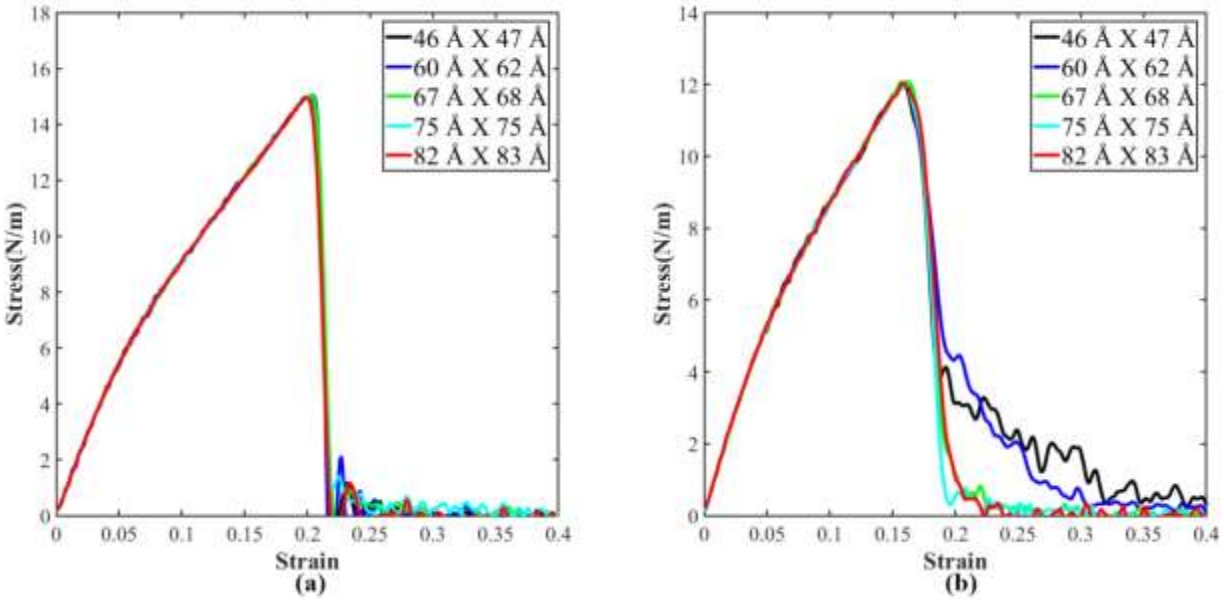

Figure S1: Effect of sample size on stress-strain curves at 300 K temperature for a) armchair loading & b) zigzag loading.

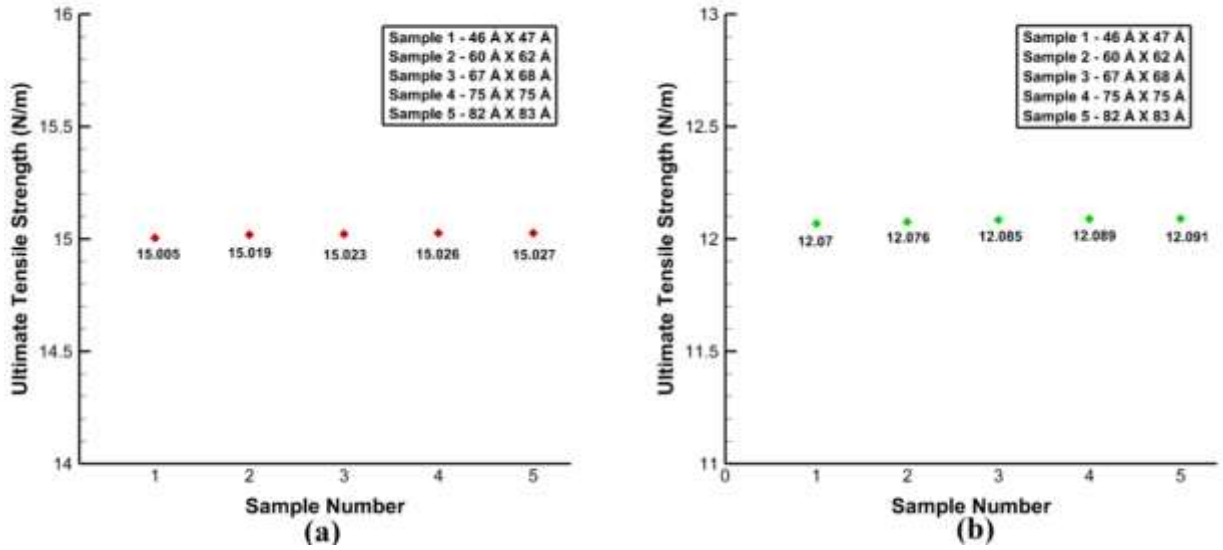

Figure S2: Convergence of UTS along with size for a) armchair loading & b) zigzag loading direction.

Section – 2

Optimized Potential Parameters:

In this study, Ge-Ge interaction has been modeled by optimized Tersoff potential[1] as below:

$$E = \sum E = \frac{1}{2}\sum_{i \neq j} V_j, \quad V_j = f(r_j)\,[\,f(r_j) + b_j\, f(r_j)]\,; \qquad 1(a)$$

$$f(r_j) = A e^{(-\lambda 1 r_{ij})}, \qquad f(r_j) = -B e^{(-\lambda_2 r_{ij})}\,; \qquad 1(b)$$

$$f(r_j) = \begin{cases} 1, & r_j < R - D \\ \frac{1}{2} - \frac{1}{2}\sin\left(\frac{\pi(r_{ij} - R)}{2}\right), & R - D < r_j < R + D \\ 0, & r_j > R + D \end{cases}; \qquad 1(c)$$

$$_{ij} = \frac{1}{(1 + \beta^n \zeta_j^n)^{\frac{1}{2n}}}, \qquad \zeta_j = \sum_{k \neq ij} f(r_k) g(\theta_{jk}) e^{[\lambda^m (r_{ij} - r_{ik})^m]}\,; \qquad 1(d)$$

$$g(\theta_{jk}) = \gamma_{jk}\left(1 + \frac{c^2}{d^2} - \frac{c^2}{[d^2 + (cos\theta_{jk} - cos\,\theta_0)^2]}\right) \qquad 1(e)$$

where E is the total potential energy of the atomic system. Further parameter notations of Tersoff potential and values of force field parameters for Ge-Ge interactions are given in[1]. In this study, the MD (Molecular Dynamics) analysis have been performed with a wide range of cutoff distance. This range stretches from R-D to R+D as shown in Tersoff formulation equation 1(c). The parameter of D has been increased to 1.25 Å keeping the R fixed to 2.95 Å, and thus the value of smaller cutoff radius R-D is decreased to 1.7 Å and the value of larger cutoff radius R+D is increased to 4.2 Å. This parametric analysis is adopted to match the derived mechanical properties of monolayer germanene (UTS and fracture stain) with the DFT results.[2]

In Tersoff potential, the cutoff function introduces a dramatic increase in the interatomic force which rises sharply with a peak at around 30% strain[3–5]. Similar phenomenon has been observed in this study when the parameter of D=0.15 was used with optimized Tersoff potential following Mahdizadeh[1], and also with D=0.30 maintaining the original Tersoff potential parameter[6] (as shown in Figure S3). Such an unphysical strain hardening is attributed to the sharply discontinuous second derivative of the Tersoff cutoff function at the cutoff activation point.

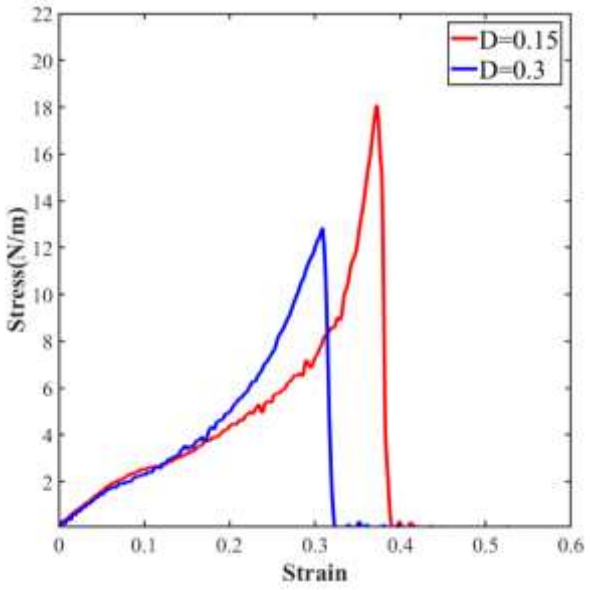

Figure S3: Stress-strain curves for armchair loading with original Tersoff parameter (D=0.3) and optimized Tersoff parameter (D=0.15).

To solve this overestimation, at first a hard cutoff of R-D=R+D=2.95 Å was chosen (considering D=0) following the methodology of many studies[3,7]. In order to validate the properties obtained from this approach with DFT study on germanene[2], tensile simulation in a single layer of germanene was performed at a strain rate of 0.003 ps^{-1} and at 300 K temperature. With this approach, the abrupt strain hardening was avoided but the mechanical properties (strength and fracture strain) were found to be much lower than the DFT calculations as shown in Table S1.

Table S1: Mechanical properties of monolayer germanene obtained from different methods

Methodology	UTS		Fracture Strain	
	Armchair	Zigzag	Armchair	Zigzag
D= 0	2.91	2.95	12.69	15.1
D=1.25	5.66	6.02	16.32	17.73
DFT[2]	4.7	4.1	20	20.5
M.Qui.Le [8]	4.6	5.1	15.9	21.4

This type of reduction in mechanical properties resulting from using a hard cutoff has also been reported in the study of Gamboa et al[9]. Moreover, even with the hard cutoff of 2.95 Å, the unexpected strain hardening was observed when we performed tensile simulations at any temperature below 300 K. The similar scenario also occurred when the value of hard cutoff was enhanced from R=2.95 Å to R=3.50 Å as shown in Figure S4. This motivated us to prepare a detail mapping of the variability of mechanical properties (UTS) with the variation of the cutoff range as shown in Figure S5. Such a range (=2D), when short as in D=0.6[1] and D=0.3[6], abruptly alters mechanical property (UTS) due to a highly steep slope in stress strain diagram near the cutoff activation point[10] **.** Therefore, when the range is widened(the value of D is increased), this unexpected strain hardening gradually goes away[11]. Moreover, increment in the larger cutoff, also helps to decrease the force overestimation[12]. It is also observed a similar conclusion from the mapping of UTS with a wide range of cutoff distance. It was also observed from Figure S5 that

the UTS value first shoots up as the value of D is changed from D=0. Then, the value of UTS gradually decreases with increasing D with converging the results for the values D>1. Moreover, this study finds that with D=1.25 the UTS and the fracture strain results match with that of the DFT calculation. It is further noted that, the value of Young's Modulus does not change significantly with variation of D because the influence of change of D is basically observed after the cutoff activation point. This approach only suppresses the spurious strength otherwise achieved through the conventional parameters.

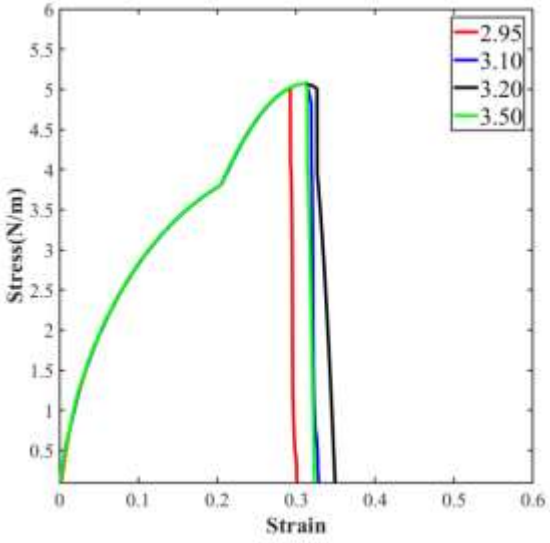

Figure S4: stress-strain curves for armchair loading with different values of hard cutoff at 5 K.

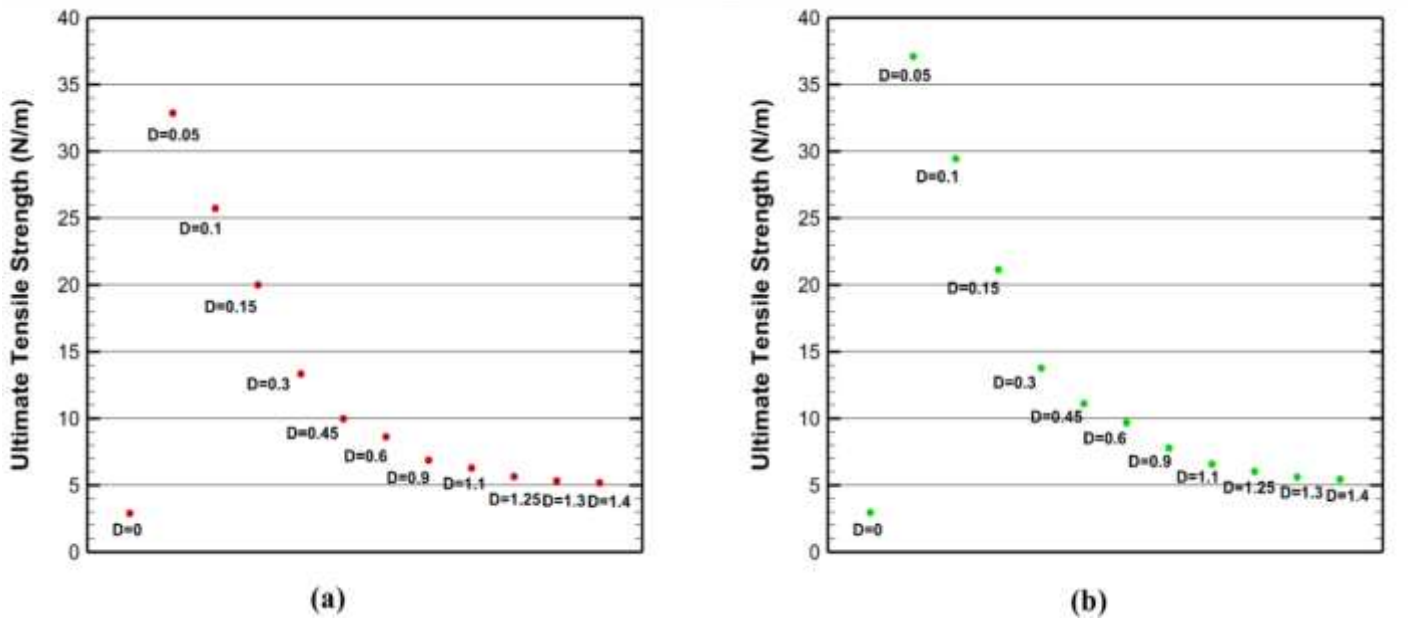

Figure S5: Effect of Tersoff parameter D on the UTS at a) armchair loading & b) zigzag loading.

1. Mahdizadeh SJ, Akhlamadi G. Optimized Tersoff empirical potential for germanene. J Mol Graph Model. 2017 Mar 1;72:1–5.

2. Mortazavi B, Rahaman O, Makaremi M, Dianat A, Cuniberti G, Rabczuk T. First-principles investigation of mechanical properties of silicene, germanene and stanene. Phys E Low-Dimens Syst Nanostructures. 2017 Mar 1;87:228–32.

3. Belytschko T, Xiao SP, Schatz GC, Ruoff RS. Atomistic simulations of nanotube fracture. Phys Rev B. 2002 Jun 20;65(23):235430.

4. Shenderova OA, Brenner DW, Omeltchenko A, Su X, Yang LH. Atomistic modeling of the fracture of polycrystalline diamond. Phys Rev B. 2000 Feb 1;61(6):3877–88.

5. Le M-Q, Batra RC. Mode-I stress intensity factor in single layer graphene sheets. Comput Mater Sci. 2016 Jun 1;118:251–8.

6. Tersoff J. Modeling solid-state chemistry: Interatomic potentials for multicomponent systems. Phys Rev B. 1989 Mar 15;39(8):5566–8.

7. Kumar R, Rajasekaran G, Parashar A. Optimised cut-off function for Tersoff-like potentials for a BN nanosheet: a molecular dynamics study. Nanotechnology. 2016 Jan;27(8):085706.

8. Le M-Q. Fracture of monolayer germanene: A molecular dynamics study. Int J Mod Phys B. 2018 Jul 27;32(22):1850241.

9. Gamboa A, Farbos B, Aurel P, Vignoles GL, Leyssale J-M. Mechanism of strength reduction along the graphenization pathway. Sci Adv. 2015 Nov 1;1(10):e1501009.

10. Powell D. Elasticity, Lattice Dynamics and Parameterisation Techniques for the Tersoff Potential Applied to Elemental and Type III-V Semiconductors. 2006.

11. Jäger HU, Albe K. Molecular-dynamics simulations of steady-state growth of ion-deposited tetrahedral amorphous carbon films. J Appl Phys. 2000 Jun 28;88(2):1129–35.

12. Huhtala M, Krasheninnikov AV, Aittoniemi J, Stuart SJ, Nordlund K, Kaski K. Improved mechanical load transfer between shells of multiwalled carbon nanotubes. Phys Rev B. 2004 Jul 7;70(4):045404.

Section – 3

Error Analysis:

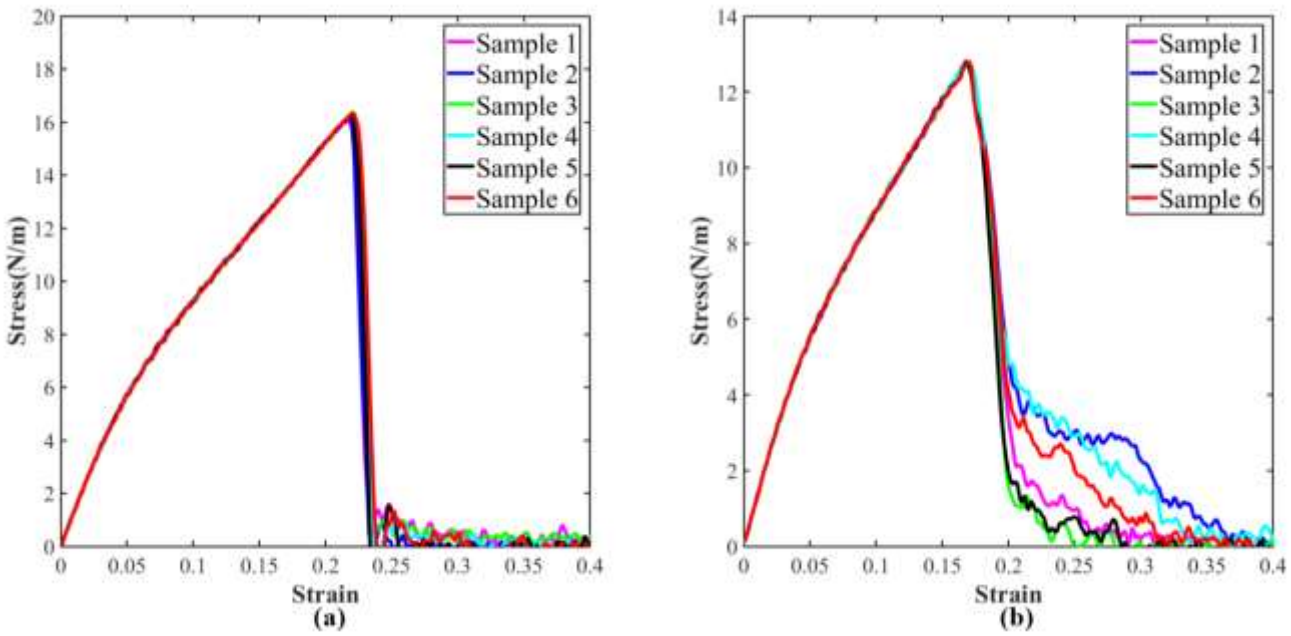

Figure S6: Stress-strain curves for six different samples with different initial velocity seeds at 200 K for a) armchair loading & b) zigzag loading.

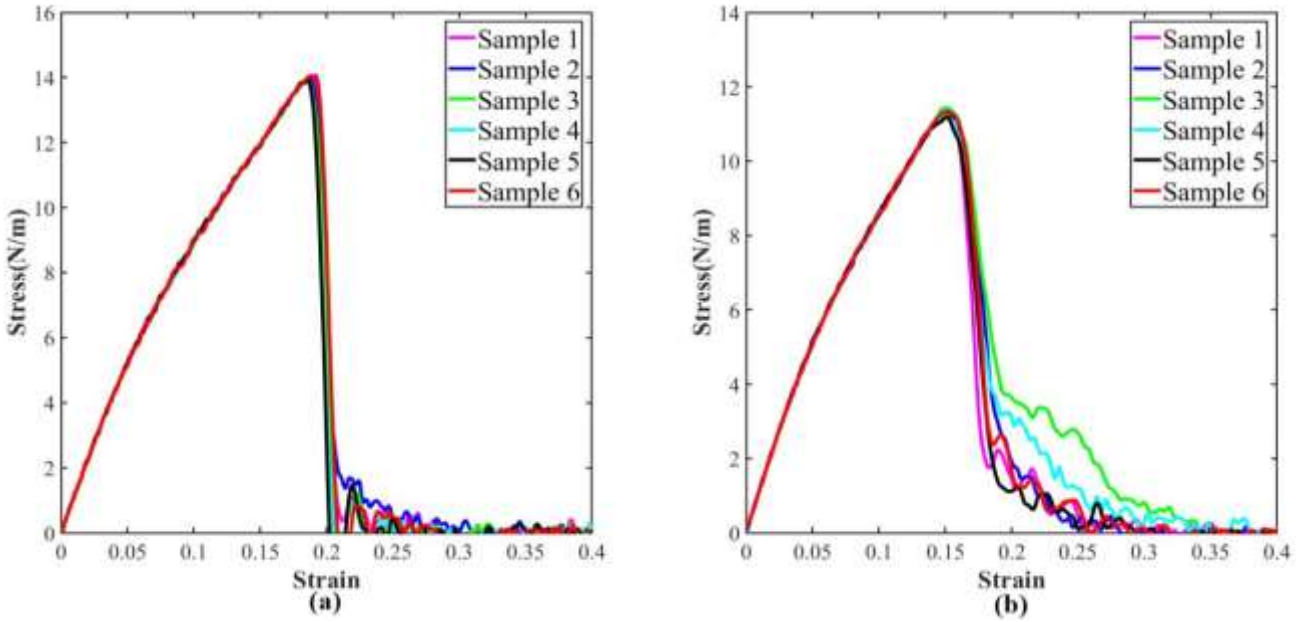

Figure S7: Stress-strain curves for six different samples with different initial velocity seeds at 400 K for a) armchair loading & b) zigzag loading.

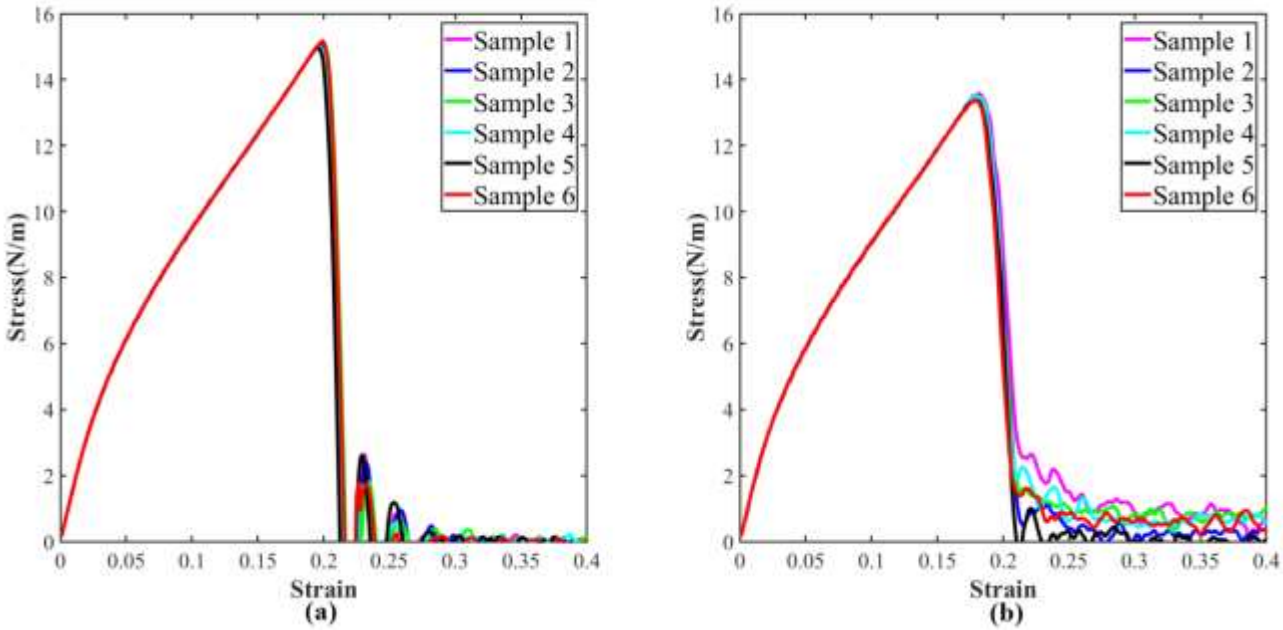

Figure S8: Stress-strain curves for six different samples having monovacancy with different initial velocity seeds at 25 K for a) armchair loading & b) zigzag loading.

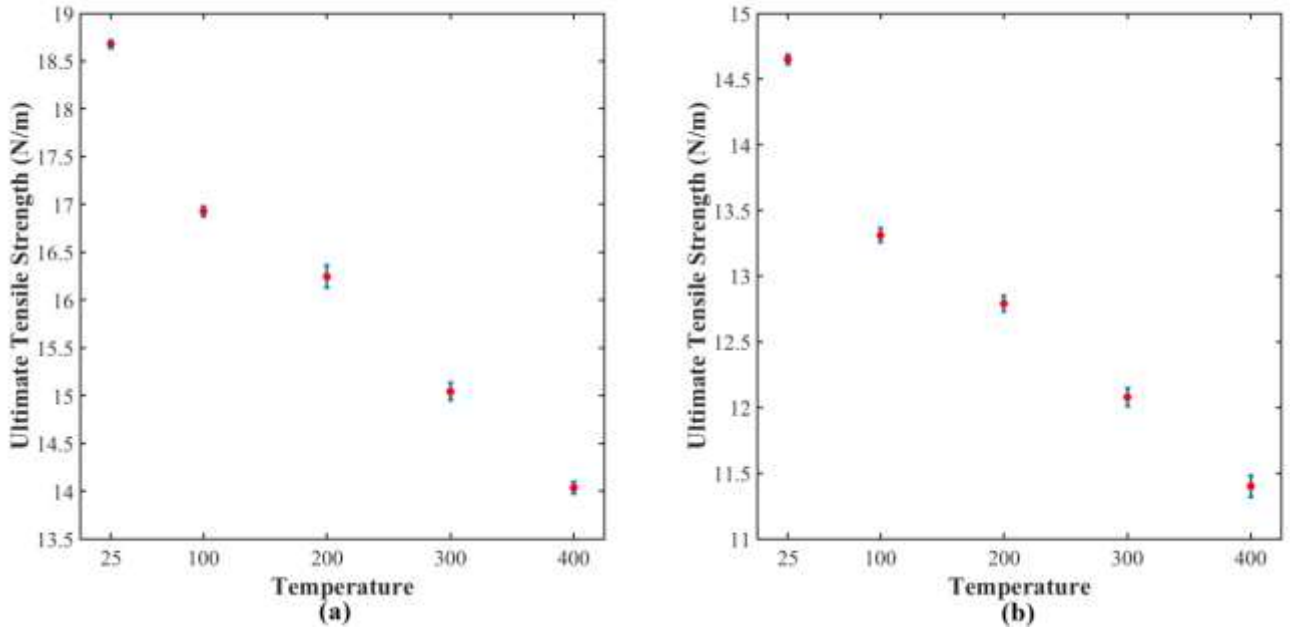

Figure S9: Errors associated to ultimate tensile strength with different initial velocity seeds at various temperatures for (a) armchair loading & (b) zigzag loading.